RSC Advances

PAPER

View Article Online
View Journal | View Issue

Check for updates

Cite this: *RSC Adv.*, 2018, **8**, 13578

Extension and functionalization of an encapsulating macrobicyclic ligand using palladium-catalyzed Suzuki–Miyaura and Sonogashira reactions of iron(II) dihalogenoclathrochelates with inherent halogen substituents†‡

Irina N. Denisenko,[a] Oleg A. Varzatskii,[a] Roman A. Selin,[ae] Alexander S. Belov,[b] Ekaterina G. Lebed,[b] Anna V. Vologzhanina,[b] Yan V. Zubavichus[d] and Yan Z. Voloshin*[bc]

A new approach for performing Suzuki–Miyaura and Sonogashira reactions of iron(II) dihalogenoclathrochelates, optimizing their reaction conditions (such as temperature, solvent and a palladium-containing catalyst) and the nature of other reagents (such as arylboron components) is elaborated. These palladium-catalyzed reactions are very sensitive to the nature of the macrobicyclic substrates. The reactivity of the leaving halogen atoms correlates with their ability to undergo an oxidative addition, decreasing in the order: I > Br > Cl, and iron(II) diiodoclathrochelate underwent these C–C cross-couplings under their "classical" conditions. Phenylboronic, 4-carboxyphenylboronic and 6-ethoxy-2-naphthylboronic acids, and the diethyl ether of 4-(ethoxycarbonyl)boronic acid were tested as components of Suzuki–Miyaura reactions in DMF and in THF. The highest yields of the target products were obtained in DMF, while the highest activation was observed with sodium and potassium carbonates. The Suzuki–Miyaura reaction of a diiodoclathrochelate with 6-ethoxy-2-naphthylboronic acid gave the mono- and difunctionalized clathrochelates resulting from the tandem hydrodeiodination – C–C cross-coupling and double C–C cross-coupling reactions, respectively. Its Sonogashira reactions with trimethylsilylacetylene and acetylenecarboxylic acid in THF and in DMF were tested. This palladium-catalyzed reaction with a $(CH_3)_3Si$-containing active component gave the target products in a high total yield. The complexes obtained were characterized using elemental analysis, MALDI-TOF, UV-Vis, ^1H and $^{13}C\{^1H\}$ NMR spectroscopy, and by single crystal XRD. Despite the non-equivalence of the ribbed α-dioximate fragments of their molecules, the encapsulated iron(II) ion is situated almost in the centre of its FeN_6-coordination polyhedron, the geometry of which is almost intermediate between a trigonal prism and a trigonal antiprism.

Received 1st March 2018
Accepted 22nd March 2018

DOI: 10.1039/c8ra01819g

rsc.li/rsc-advances

Open Access Article. Published on 11 April 2018. Downloaded on 7/15/2024 4:41:03 AM.
This article is licensed under a Creative Commons Attribution-NonCommercial 3.0 Unported Licence.

Introduction

The designed cage metal complexes[1,2] have been widely used for the design and preparation of prospective drug candidates {so-called "topological drugs", such as antiviral, antitumor (including cytostatic[3]) and antifibrillogenic prodrugs; the main results in this field have been highlighted recently[4]}, for efficient electro(pre)catalysts of the hydrogen evolution reaction $2H^+/H_2$ in aqueous solutions,[2,5–7] as mediators of electron transfer for electrochemical sensors, as macrobicyclic precursors and components of molecular electronic devices, such as molecular switches[2] and quantum gates,[8,9] as paramagnetic probes,[2] as well as mononuclear single-molecule magnets with record characteristics,[10,11] and are thus prospective magnetic

[a]*Vernadskii Institute of General and Inorganic Chemistry NASU, 03142 Kiev, Ukraine*
[b]*Nesmeyanov Institute of Organoelement Compounds RAS, 119991 Moscow, Russia. E-mail: voloshin@ineos.ac.ru*
[c]*Kurnakov Institute of General and Inorganic Chemistry RAS, 119991 Moscow, Russia*
[d]*Kurchatov Complex for Synchrotron and Neutron Investigations, National Research Centre Kurchatov Institute, 123182 Moscow, Russia*
[e]*PBMR Labs Ukraine, 02094 Kiev, Ukraine*

† Other authors dedicate this paper to the memory of Prof. O. Varzatskii who suddenly passed away on 20 December 2017.

‡ Electronic supplementary information (ESI) available. CCDC 1825075–1825077. For ESI and crystallographic data in CIF or other electronic format see DOI: 10.1039/c8ra01819g

This journal is © The Royal Society of Chemistry 2018

Open Access Article. Published on 11 April 2018. Downloaded on 7/15/2024 4:41:03 AM.
This article is licensed under a Creative Commons Attribution-NonCommercial 3.0 Unported Licence.

materials. So, one of the main aims of their chemistry is the development of highly efficient methods of straightforward synthesis of functionalized cage metal complexes with a given size, position and reactivity of the functionalizing substituents using suitable clathrochelate precursors as molecular platforms (scaffolds), those of the hybrid systems based on them and of macrobicyclic ligands with a given geometry, possessing the given physical, physicochemical (including redox and electrocatalytic) and donor ability. Metal-catalyzed C–C cross-couplings (in particular, the Suzuki–Miyaura and Sonogashira reactions) are powerful synthetic methods in modern organic chemistry, whereas the reactivity of the coordinated ligands in their metal complexes has very rarely been used in coordination chemistry to date. In particular, the Sonogashira reactions of the ethynyl-terminated apically functionalized iron(II) clathrochelates have been used[12] for further extension of their substituents at capping boron atoms. Metal tris–dioximate halogenoclathrochelates are reported[1,2] to be the key reactive macrobicyclic precursors for the design and preparation of these metal-centered compounds, as well as of the polynuclear and hybrid systems, coordination cages, coordination polymers, and MOFs based on them. Earlier, several metal-promoted (catalyzed) reactions of such halogenoclathrochelate precursors shown in Scheme 1 and 2 were performed. They include cadmium-promoted *N*,*C*,*O*-nucleophilic substitution (**1**, Scheme 1), as well as copper-promoted reactions of cyanation–hydrodehalogenation (**2**, Scheme 1), perfluoroalkylation (**3**, Scheme 1), perfluoroarylation (**4**, Scheme 1), halogen exchange (**5**, Scheme 2) and reductive C–C homocoupling (**6**, Scheme 2).[2] We have also performed[13] the palladium-catalyzed Suzuki–Miyaura and Sonogashira reactions of hybrid α-furyldioximate–α-benzildioximate monoribbed-functionalized iron(II) dibromoclathrochelate, the molecule from which contains reactive bromine atoms in its α-furyl ribbed substituents (**7**, Scheme 2). Therefore, these C–C cross-couplings can be regarded as purely organic reactions due to the remoteness of their reactive centers from the cage framework (and, therefore, from the encapsulated metallocenter). On the other hand, the Suzuki–Miyaura and Sonogashira reactions of iron(II) dihalogenoclathrochelates with inherent halogen substituents, which are directly bound to a polyazomethine quasiaromatic macrobicyclic framework, seem to be affected by the nature of these macrobicyclic substrates and, therefore, the above reactions should have some peculiarities in the order of their reactive halogen atoms (*i.e.* Cl, Br and I). In particular, the iron(II) dichloro- and dibromoclathrochelates are reported[14] to be much less reactive (or, even, unreactive) in their palladium-catalyzed and copper-promoted C-carboranylation reactions shown in Scheme 2, **8** as compared with their iodine-containing macrobicyclic analogs. Moreover, the latter reaction gave only the product of its tandem C-carboranylation–hydrodehalogenation transformation, the first hybrid monocarboranoclathrochelate with methine hydrogen atom in the *vic*-position of the functionalizing polyhedral substituent. In general, almost all the above copper-promoted substitution, exchange and homocoupling processes were accompanied by consecutive hydrodehalogenation and tandem hydrodehalogenation–homocoupling side reactions (Scheme 2, **9**), and by the complete destruction of the cage framework (especially under basic reaction conditions) as well. As a result, the total yield of the target macrobicyclic products of these C–C couplings typically did not exceed 20%. In this paper, we describe our attempts to evaluate a new approach for performing Suzuki–Miyaura and Sonogashira cross-coupling reactions of iron(II) dihalogenoclathrochelates as macrobicyclic substrates that optimizes the reaction conditions (such as temperature, solvent and use of palladium-containing catalyst), as well as the nature of other reagents (such as the arylboron components), thus trying to increase the yield of the target functionalized clathrochelate product and to avoid the above side reactions. We also aimed to obtain the first functionalized iron(II) clathrochelates with terminal triple C≡C bonds, which may be used for further functionalization (in particular, using the very common organic "click"-reactions).

Experimental

General considerations

The reagents used, phenylboronic, acetylenecarboxylic and 6-ethoxy-2-naphthylboronic acids, the diethyl ether of 4-

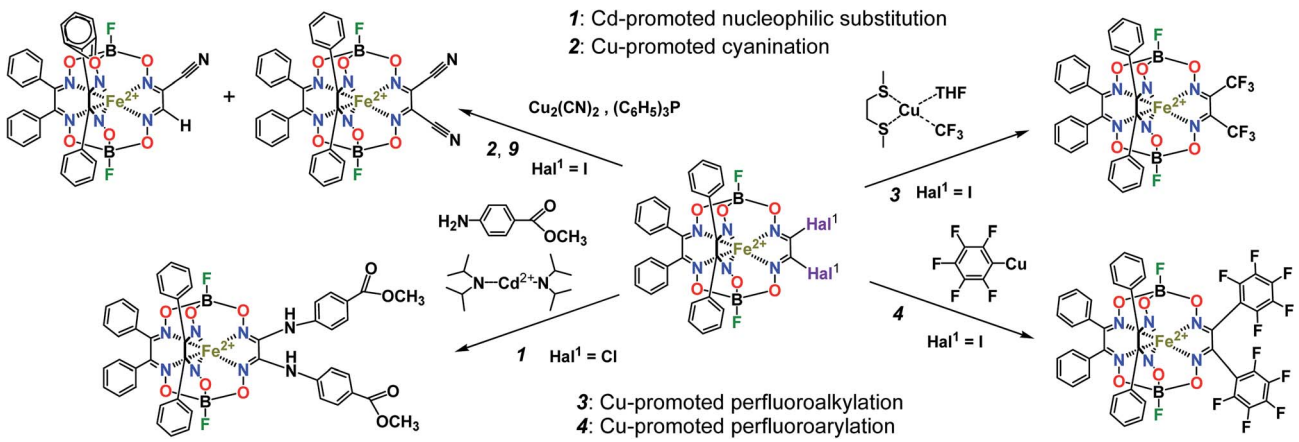

Scheme 1 Cadmium- and copper-promoted reactions of the iron(II) halogenoclathrochelates.

Open Access Article. Published on 11 April 2018. Downloaded on 7/15/2024 4:41:03 AM.
This article is licensed under a Creative Commons Attribution-NonCommercial 3.0 Unported Licence.

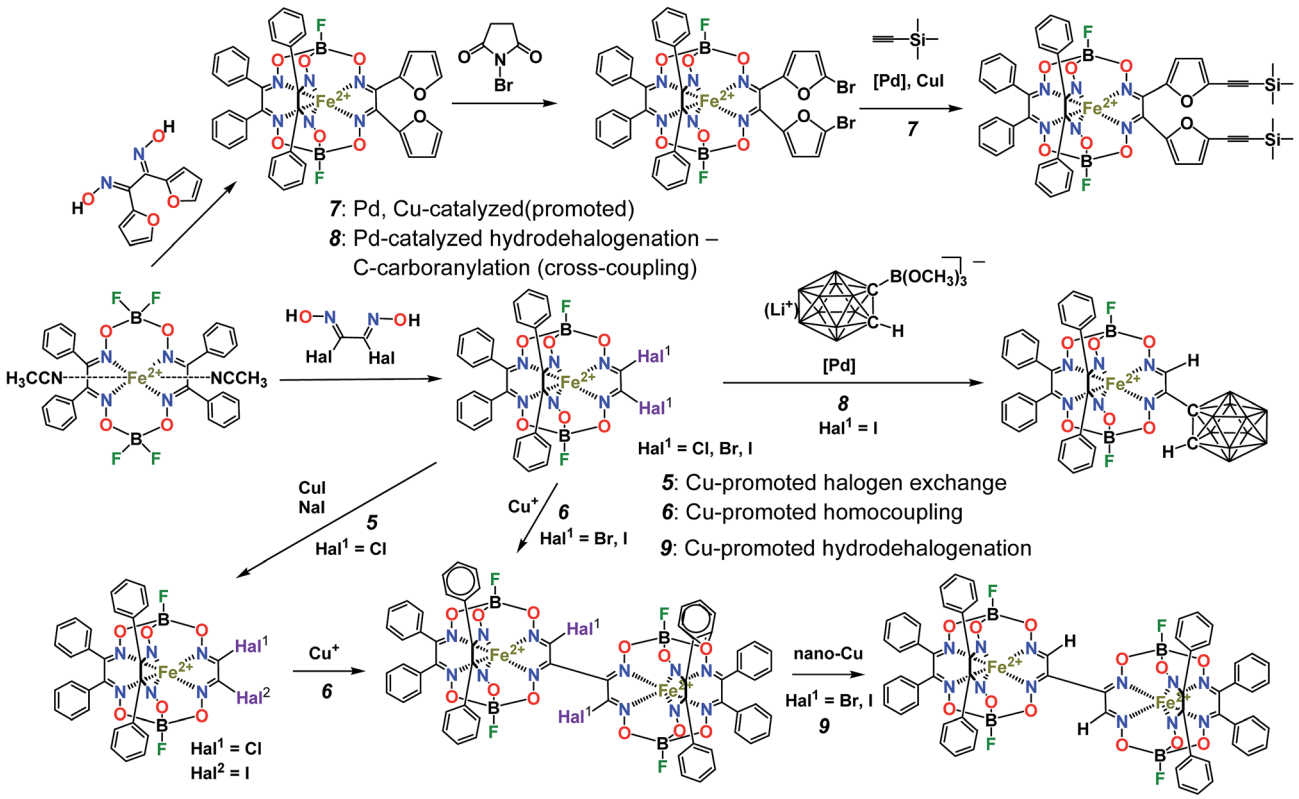

Scheme 2 Metal-promoted (catalyzed) reactions of iron(II) halogenoclathrochelates and their derivatives.

(ethoxycarbonyl)phenylboronic acid, trimethylsilylacetylene, complex Pd(dppf)Cl_2 (where dppf is 1,1′-ferrocenediyl-bis(diphenylphosphine)), copper(I) iodide, triethylamine, sorbents, bases, and organic solvents were obtained commercially (Sigma-Aldrich®). The dihalogenoclathrochelates $FeBd_2(I_2Gm)(BF)_2$ (**7**), $FeBd_2(Cl_2Gm)(BF)_2$ (**8**) and $FeBd_2(Br_2Gm)(BF)_2$ (**9**) were obtained as described elsewhere.[1,2]

Analytical data (C, H, N contents) were obtained with a Carlo Erba model 1106 microanalyzer.

MALDI-TOF mass spectra were recorded in both the positive and the negative spectral regions using a MALDI-TOF-MS Bruker Autoflex mass spectrometer in reflecto-mol mode. The ionization was induced by a UV-laser with a wavelength of 336 nm. The sample was applied to a nickel plate, and 2,5-dihydroxybenzoic acid was used as a matrix. The accuracy of the measurements was 0.1%.

UV-Vis spectra of the solutions in dichloromethane were recorded in the range 230–800 nm with a Varian Cary 50 spectrophotometer. The individual Gaussian components of these spectra were calculated using the Fityk program.[15]

^1H, $^{13}C\{^1H\}$, $^{19}F\{^1H\}$ and $^{11}B\{^1H\}$, as well as 2D COSY, HSQC and HMBC, NMR spectra of the complexes obtained were recorded from their CD_2Cl_2 solutions using Bruker Avance 400 and Bruker Avance 600 spectrometers. The measurements were done using the residual signals of CD_2Cl_2: ^1H 5.32 ppm, ^{13}C 54.00 ppm. ^1H and ^{13}C chemical shifts are reported in ppm downfield from TMS. ^{19}F and ^{11}B NMR chemical shifts were referenced to the external $CFCl_3$ and $BF_3 \cdot OEt_2$, respectively.

Synthesis

Preparation of $FeBd_2((EtONaphth)_2Gm)(BF)_2$ (1) and $FeBd_2(EtONaphthGmH)(BF)_2$ (2). Complex $FeBd_2(I_2Gm)(BF)_2$ (**7**, 0.233 g, 0.249 mmol) was dissolved in DMF (10 ml), and 1 ml of Na_2CO_3 aqueous solution (0.119 g, 1.125 mmol) and 6-ethoxynaphthaleneboronic acid (0.135 g, 0.625 mmol) were added. Then the reaction mixture was deaerated using three pumping-argon saturation cycles and complex Pd(dppf)Cl_2 (0.009 g, 0.013 mmol) was added. The reaction mixture was stirred for 15 min at r.t., then heated to 90 °C and stirred at this temperature for 10 h. The obtained dark-red mixture was cooled to r.t. and rotary evaporated to dryness. The solid residue was treated with water (10 ml) and filtered off. The precipitate was washed with water, dried in air and extracted with dichloromethane (10 ml). The extract was flash-chromatographically purified on silica gel (30 mm layer, eluent: dichloromethane); the eluate was evaporated to a small volume and precipitated with hexane (50 ml). The precipitate was filtered off, washed with hexane and dried *in vacuo*. The solid product was separated using column chromatography on Silasorb 300 (eluent: dichloromethane–hexane 1 : 2 mixture). Two major red eluates were evaporated to dryness, washed with hexane and dried *in vacuo*.

*$FeBd_2((EtONaphth)_2Gm)(BF)_2$ (first eluate, **1**).* Yield: 0.023 g (9%). Calc. for $C_{54}H_{42}N_6B_2F_2O_8Fe$: C, 63.69; H, 4.16; N, 8.25. Found (%): C, 63.68; H, 4.34; N, 8.35. MS (MALDI-TOF): *m*/*z*: 1018 $[M]^+$. ^1H NMR (CD_2Cl_2, δ, ppm): 1.44 (t, $^3J_{HH}$ = 7.0 Hz, 6H, CH_3), 4.12 (q, $^3J_{HH}$ = 7.0 Hz, 4H, CH_2), 7.08 (d, $^4J_{HH}$ = 2.4 Hz, 2H, napht), 7.09 (dd, $^3J_{HH}$ = 8.7 Hz, $^4J_{HH}$ = 2.4 Hz, 2H, napht),

 This journal is © The Royal Society of Chemistry 2018

Open Access Article. Published on 11 April 2018. Downloaded on 7/15/2024 4:41:03 AM.
This article is licensed under a Creative Commons Attribution-NonCommercial 3.0 Unported Licence.

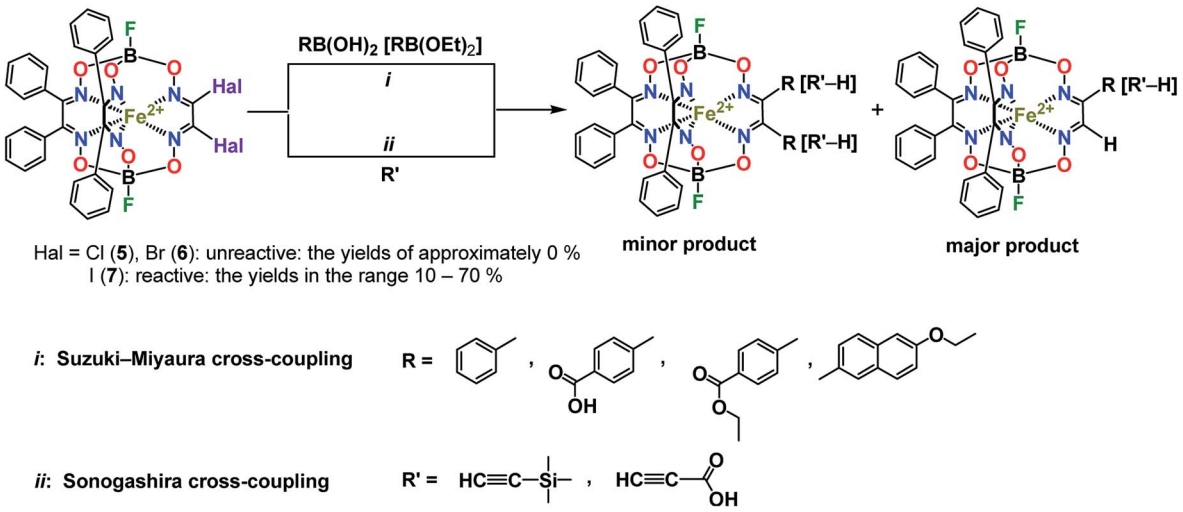

Scheme 3 The tested palladium-catalyzed Suzuki–Miyaura and Sonogashira reactions of iron(II) dihalogenoclathrochelates.

7.32–7.42 (m, 14H, *meta*-Ph, *para*-Ph, napht), 7.45 (d, $^3J_{HH}$ = 7.0 Hz, 8H, *ortho*-Ph), 7.58(d, $^3J_{HH}$ = 8.7 Hz, 2H, napht), 7.62 (d, $^3J_{HH}$ = 8.8 Hz, 2H, napht), 8.04 (d, $^3J_{HH}$ = 1.3 Hz, 2H, napht). $^{13}C\{^1H\}$ NMR (CD_2Cl_2, δ, ppm): 15.04 (s, CH_3), 64.22 (s, CH_2), 106.84, 120.24, 124.93, 126.63, 127.98 (all s, napht), 128.56, 129.83, 130.72 (all s, Ph), 130.75, 131.12, 131.19 (all s, napht), 131.26 (s, Ph), 132.02, 135.72 (both s, napth), 157.35 (s, PhC=N), 159.16 (s, naphthC=N). UV-Vis (CH_2Cl_2), λ_{max}, nm($\varepsilon\cdot10^{-3}$, mol^{-1} l cm^{-1}): 237(82), 286(33), 328(14), 343(1.7), 375(7.6), 411(1.4), 479(29), 494(8.5).

*$FeBd_2$(EtONaphthGmH)$(BF)_2$ (second eluate, **2**).* Yield: 0.154 g (60%). Calc. for $C_{42}H_{32}N_6B_2F_2O_7Fe$: C, 59.47; H, 3.80; N, 9.91. Found (%): C, 59.56; H, 3.75; N, 9.76. MS (MALDI-TOF): *m*/*z*: 848 $[M]^{+\bullet}$. ^1H NMR (CD_2Cl_2, δ, ppm): 1.48 (t, $^3J_{HH}$ = 7 Hz, 3H, CH_3), 4.19 (q, $^3J_{HH}$ = 7 Hz, 2H, CH_2), 7.20 (d, $^4J_{HH}$ = 2.5, 1H, napht), 7.21 (dd, $^3J_{HH}$ = 8.7 Hz, $^4J_{HH}$ = 2.5 Hz, 1H, napht), 7.32–7.42 (m, 21H, Ph, napht), 7.85 (d, $^3J_{HH}$ = 8.7 Hz, 1H, napht), 7.86 (d, $^3J_{HH}$ = 8.7 Hz, 1H, napht), 8.01 (dd, $^3J_{HH}$ = 8.7, $^4J_{HH}$ = 1.9 Hz, 1H, napht), 8.46 (s, 1H, HC=N). $^{13}C\{^1H\}$ NMR (CD_2Cl_2, δ, ppm): 15.07 (s, CH_3), 64.34 (s, CH_2), 106.93, 120.72, 124.20, 126.67, 127.70, 128.50 (all s, napht), 128.57 (m, *meta*-Ph + napht), 128.61 (s, *meta*-Ph), 129.69, 129.76 (both s, *ipso*-Ph), 130.75 (s, *para*-Ph), 131.12, 131.19 (both m, *ortho*-Ph + napht), 136.34 (s, napht), 146.47 (s, HC=N), 156.90 (s, PhC=N), 157.23 (s, PhC=N), 159.59 (s, naphthC=N). UV-Vis (CH_2Cl_2), λ_{max}, nm($\varepsilon\cdot10^{-3}$, mol^{-1} l cm^{-1}): 235(60), 258(24), 281(33), 311(7.3), 338(7.7), 372(6.3), 470(18), 484(15).

Preparation of $FeBd_2$(((Me$_3$Si)C≡C)$_2$Gm)$(BF)_2$ (3) and $FeBd_2$((Me$_3$Si)C≡CGmH)$(BF)_2$ (4). Complex $FeBd_2(I_2Gm)(BF)_2$ (7, 0.325 g, 0.347 mmol) was dissolved/suspended in THF (15 ml), and copper(I) iodide (0.033 g, 0.175 mmol), trimethylsilylacetylene (0.25 ml, 1.75 mmol) and triethylamine (0.1 ml, 1.35 mmol) were added. The reaction mixture was deaerated using the above pumping-saturation procedure and complex Pd(dppf)Cl_2 (0.013 g, 0.017 mmol) was added. The reaction mixture was stirred for 30 min at r.t. and then for 6 h at 50 °C. The obtained dark-red solution/suspension was cooled to r.t., rotary evaporated to dryness and dried *in vacuo*. The solid residue was extracted with dichloromethane (50 ml), the extract was washed with water (40 ml, in two portions), dried with $MgSO_4$ and flash-chromatographically purified on silica gel (20-mm layer, eluent: dichloromethane). The eluate was evaporated to a small volume and precipitated with hexane (50 ml). The precipitate was filtered off, washed with hexane and dried *in vacuo*. The solid product was separated column chromatographically on Silasorb 300 (eluent: dichloromethane–hexane 1 : 3 mixture). Two major eluates were collected, evaporated to dryness, washed with hexane and dried *in vacuo*.

*$FeBd_2$(((Me$_3$Si)C≡C)$_2$Gm)$(BF)_2$. (first eluate, **3**).* Yield: 0.046 g (15%). Calc. for $C_{40}H_{38}N_6B_2F_2O_6Si_2Fe$: C, 55.20; H, 4.40; N, 9.66. Found (%): C, 55.08; H, 4.29; N, 9.75. MS (MALDI-TOF): *m*/*z*: 870 $[M]^{+\bullet}$. ^1H NMR (CD_2Cl_2, δ, ppm): 0.31 (s, 18H, Me_3Si), 7.36 (m, 20H, Ar). $^{13}C\{^1H\}$ NMR (CD_2Cl_2, δ, ppm): −0.44 (s, Me_3Si), 101.16, 109.62 (two s, C≡C), 128.60, 129.54, 130.85, 131.09 (all s, Ph), 157.01 (s, C≡C–C=N), 157.15 (s, PhC=N). ^{11}B NMR (CD_2Cl_2, δ, ppm): 3.78 (d, $J_{^{11}B-^{19}F} \approx 15$ Hz). ^{19}F NMR (CD_2Cl_2, δ, ppm): −168.62 (m). UV-Vis (CH_2Cl_2), λ_{max}, nm($\varepsilon\cdot10^{-3}$, mol^{-1} l cm^{-1}): 263(28), 283(1.6), 296(8.5), 319(5.5), 341(3.4), 343(8.6), 478(10), 486(12), 523(10).

*$FeBd_2$((Me$_3$Si)C≡CGmH)$(BF)_2$. (second eluate, **4**).* Yield: 0.213 g (70%). Calc. for $C_{35}H_{30}N_6B_2F_2O_6SiFe$: C, 54.30; H, 3.91; N, 10.86. Found (%): C, 54.21; H, 4.06; N, 10.71. MS (MALDI-TOF): *m*/*z*: 774 $[M]^{+\bullet}$. ^1H NMR (CD_2Cl_2, δ, ppm): 0.32 (s, 9H, Me_3Si), 7.36 (m, 20H, Ph), 8.04 (s, 1H, CH). $^{13}C\{^1H\}$ NMR (CD_2Cl_2, δ, ppm): −0.41 (s, Me_3Si), 95.51, 110.11 (two s, C≡C), 128.61 (br s, *meta*-Ph), 129.49, 129.51 (both s, *ipso*-Ph), 130.89 (br s, *para*-Ph), 131.06 (br s, *ortho*-Ph), 135.12 (s, C≡C–C=N), 145.71 (s, HC=N), 157.09, 157.18 (two s, PhC=N). ^{19}F NMR (CD_2Cl_2, δ, ppm): −168.6 (m). ^{11}B NMR (CD_2Cl_2, δ, ppm): 3.69(d, $J_{^{11}B-^{19}F} \approx 15$ Hz), 3.83(d, $J_{^{11}B-^{19}F} \approx 15$ Hz). UV-Vis (CH_2Cl_2), λ_{max}, nm($\varepsilon\cdot10^{-3}$, mol^{-1} l cm^{-1}): 247(36), 264(3.7), 279(3.4), 295(12), 353(2.8), 384(1.0), 453(8.6), 477(23).

Open Access Article. Published on 11 April 2018. Downloaded on 7/15/2024 4:41:03 AM.
This article is licensed under a Creative Commons Attribution-NonCommercial 3.0 Unported Licence.

X-ray crystallography

Single crystals of the complexes $FeBd_2((EtONaphth)_2Gm)(BF)_2 \cdot CH_2Cl_2$ ($\mathbf{1}\cdot 3CH_2Cl_2$), $FeBd_2((EtONaphth)_2Gm)(BF)_2$ (**1**) and $FeBd_2((Me_3Si)C{\equiv}CGmH)(BF)_2$ (**4**) were grown from dichloromethane–hexane, chloroform–heptane and benzene–*iso*-octane mixtures, respectively, by a slow evaporation of their saturated solutions at room temperature. The intensities of the reflections for crystal $\mathbf{1}\cdot 3CH_2Cl_2$ were measured at 120 K using a Bruker Apex II CCD diffractometer with Mo-Kα radiation ($\lambda = 0.71073$ Å, graphite monochromator). Those for crystals **1** and **4** were collected at 100 K at the BELOK beamline of the Kurchatov Synchrotron Radiation Source (Moscow, Russia) at a wavelength of 0.9699 Å using a Rayonix SX-165 CCD detector. The structures were solved by the direct method using SHELXTL[16] and refined by full-matrix least squares against F^2. Non-hydrogen atoms were refined in the anisotropic approximation except those for the naphthalene fragments of the ribbed functionalizing substituents of a clathrochelate molecule in the crystal $FeBd_2((EtONaphth)_2Gm)(BF)_2$ (**1**) which are equiprobably disordered over two sites. The corresponding carbon atoms were refined isotropically. The unit cell of this crystal contains the solvate molecules that have been treated as a diffuse contribution to the overall scattering without specific atom positions by SQUEEZE/PLATON.[17] Hydrogen atoms were included in the refinement using the riding model with $U_{iso}(H) = nU_{eq}(C)$, where $n = 1.5$ for methyl groups and 1.2 for other atoms. All calculations were made using the SHELXL-2014 (ref. 18) and OLEX2 (ref. 19) program packages. The main crystallographic data and experimental details for all X-rayed crystals are collected in Tables S1 (see ESI‡).

Results and discussion

The tested Suzuki–Miyaura and Sogonashira reactions of the iron(II) dihalogenoclathrochelates are shown in Scheme 3. These palladium-catalyzed C–C cross-couplings are very sensitive to the nature of the reactive halogenoclathrochelate substrates as macrobicyclic precursors. The reactivity of the leaving halogen atoms in the ribbed chelate fragments of a quasiaromatic cage framework correlates with their ability to undergo an oxidative addition leading to the formation of the corresponding organopalladium compounds; it decreases in the order: I > Br > Cl > F. This order is uncommon and specific to the above metal-promoted (catalyzed) reactions of these halogenoclathrochelates: in the case of well-known classical reactions of organic substrates, the reactivity of their leaving halogen atoms decreases in the opposite order (*i.e.* from fluorine to iodine substituents). As a result, the reactivity of the

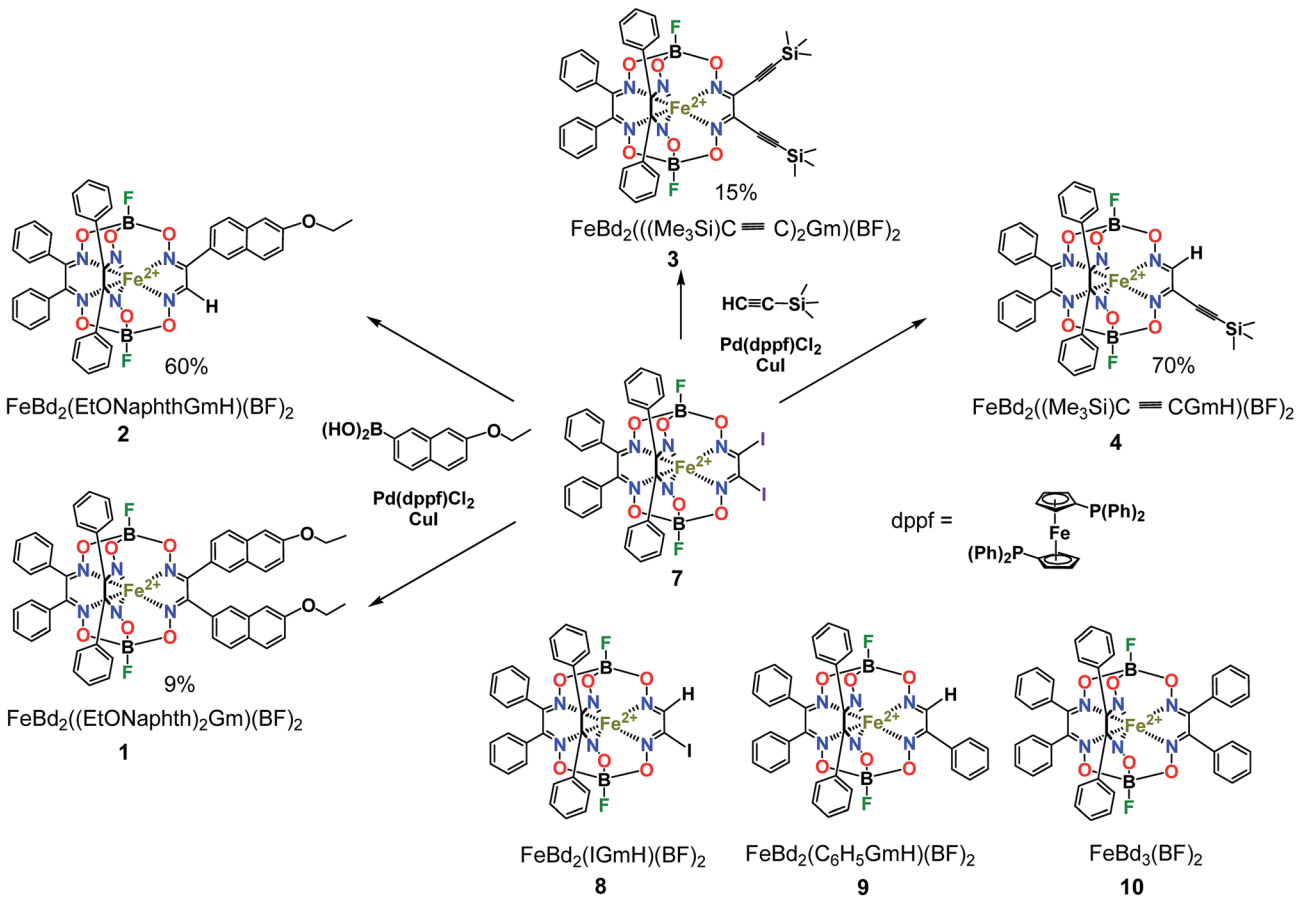

Scheme 4 Suzuki–Miyaura and Sonogashira reactions of a diiodoclathrochelate precursor and chemical drawings of the clathrochelate complexes **8**–**10** under discussion.

This journal is © The Royal Society of Chemistry 2018

Open Access Article. Published on 11 April 2018. Downloaded on 7/15/2024 4:41:03 AM.
This article is licensed under a Creative Commons Attribution-NonCommercial 3.0 Unported Licence.

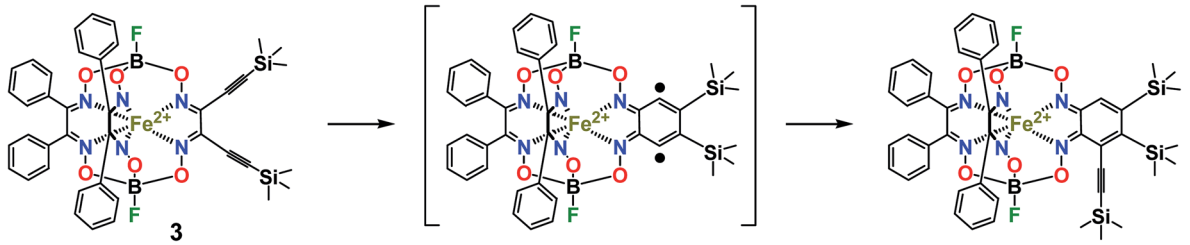

Scheme 5 Plausible pathway of chemical transformations of the *vic*-diethynyl-substituted iron(II) clathrochelate $FeBd_2(((Me_3Si)C{\equiv}C)_2Gm)(BF)_2$ (**3**) as a reactive intermediate.

iron(II) *vic*-dihalogenoclathrochelates with two inherent halogen atoms, the macrobicyclic tris-dioximate molecules of which are quasiaromatic electron-deficient systems, as the substrates in their Suzuki–Miyaura and Sonogashira reactions, decreases in the order: $FeBd_2(I_2Gm)(BF)_2$ (**7**) > $FeBd_2(Br_2Gm)(BF)_2$ (**6**) > $FeBd_2(Cl_2Gm)(BF)_2$ (**5**). Indeed, the complex $FeBd_2(Cl_2Gm)(BF)_2$ (**5**) does not undergo these C–C cross-couplings, while in the case of its dibromine-containing analog $FeBd_2(Br_2Gm)(BF)_2$ (**6**), a side reaction of the hydrolytic destruction of its cage framework occurs more quickly than the expected consecutive process of the formation of the single C–C bond between this framework and the corresponding functionalizing ribbed substituent. In contrast, the diiodoclathrochelate $FeBd_2(I_2Gm)(BF)_2$ (**7**) underwent the above palladium-catalyzed cross-couplings under their "classical" reaction conditions, thus allowing the target extension and functionalization of its encapsulating macrobicyclic ligand (Scheme 3).

For the boron-containing components of the Suzuki–Miyaura reactions of the dihalogenoclathrochelate substrates, we tested phenylboronic acid, 4-carboxyphenylboronic and 6-ethoxy-2-naphthylboronic acids, and the diethyl ether of 4-(ethoxycarbonyl)phenylboronic acid (Scheme 3); these reactions were performed both in DMF and in THF as the solvents. The highest yields of the target clathrochelate products were obtained in DMF media, while the highest activation of the above boron-containing compounds was observed in the case of Na_2CO_3 aqueous solution as an inorganic base. The attempted Suzuki–Miyaura reaction of $FeBd_2(I_2Gm)(BF)_2$ (**7**) with phenylboronic acid under these reaction conditions resulted mainly in the complete destruction of its cage framework and gave the macrobicyclic products of hydrodehalogenation and tandem hydrodehalogenation–substitution processes (the complexes

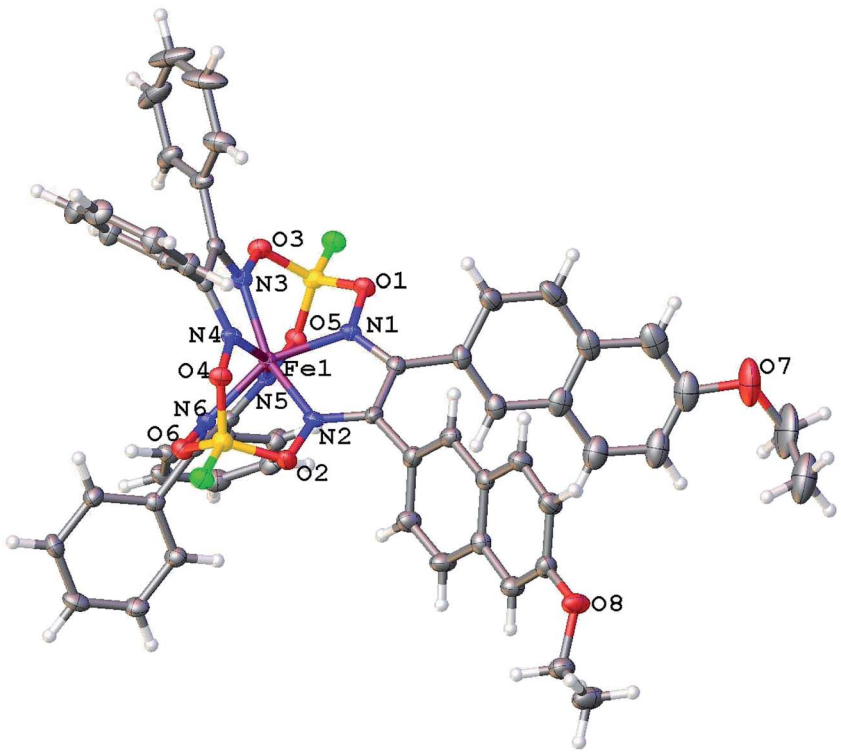

Fig. 1 General view of the molecule $FeBd_2((EtONaphth)_2Gm)(BF)_2$ (**1**) in the crystal $\mathbf{1}\cdot 3CH_2Cl_2$ in a representation of its atoms with thermal ellipsoids drawn at $p = 50\%$.

Open Access Article. Published on 11 April 2018. Downloaded on 7/15/2024 4:41:03 AM.
This article is licensed under a Creative Commons Attribution-NonCommercial 3.0 Unported Licence.

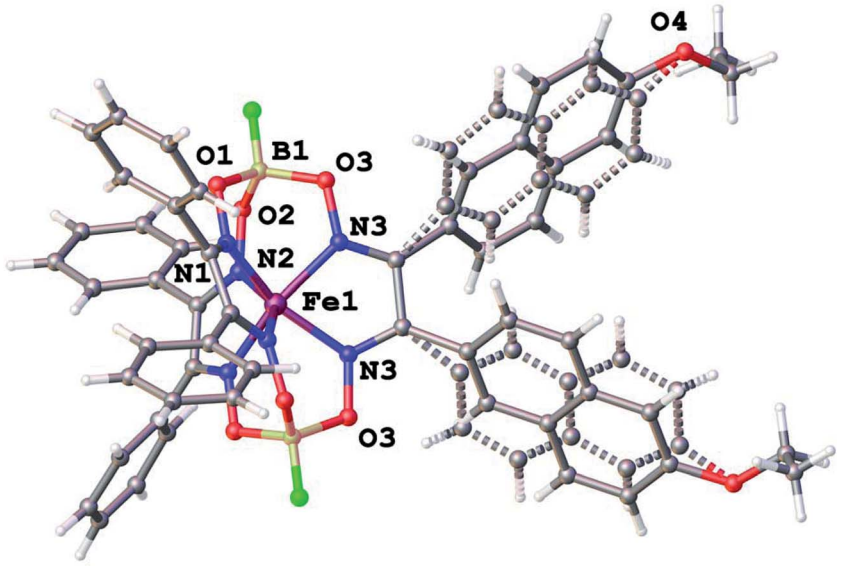

Fig. 2 General view of a clathrochelate molecule in the solvent-free crystal $FeBd_2((EtONaphth)_2Gm)(BF)_2$ (**1**). One of its two disordered fragments is depicted with dashed lines.

$FeBd_2(IGmH)(BF)_2$ (**8**) and $FeBd_2(C_6H_5GmH)(BF)_2$ (**9**), respectively), in low yields. At the same time, only trace amounts of the target diaryl-substituted clathrochelate product of this Suzuki–Miyaura reaction, a well-known[1] tris-α-benzildioximate macrobicyclic complex $FeBd_3(BF)_2$ (**10**), was detected among its products. Moreover, in the absence of phenylboronic acid, the reaction in the system $FeBd_2(I_2Gm)(BF)_2$ (**7**)–$Pd(dppf)Cl_2$–Na_2CO_3 (aq) under the same reaction conditions afforded the monomethine clathrochelate $FeBd_2(IGmH)(BF)_2$ (**8**) as the product of a side hydrodehalogenation process. The latter complex has not been described in the literature to date: indeed, its preparation using the direct template condensation of the corresponding macrocyclic bis-α-benzildioximate precursor with monoiodoglyoxime (a most promising pathway for the synthesis of the analogous monochloroclathrochelates) is hampered by the high reactivity of the above α-dioxime, which easily undergoes the side redox and substitution reactions. In the case of 4-carboxyphenylboronic acid as a boron-containing component, we failed to perform its Suzuki–Miyaura reaction with the same diiodoclathrochelate precursor: a side destruction reaction of its cage framework dominated over the expected C–C cross-coupling. On the other hand, the use of diethyl ether of 4-(ethoxycarbonyl)phenylboronic acid (as a component with an electron-withdrawing substituent), and of 6-ethoxy-2-naphthylboronic acid (its molecule contains an electron-donor substituent), allowed the target clathrochelate products of the Suzuki–Miyaura cross-coupling reaction to be obtained. In the former case, powdered K_2CO_3 was used as an inorganic base instead of Na_2CO_3 aqueous solution to avoid a cleavage of the ester group. The Suzuki–Miyaura cross-coupling reaction of $FeBd_2(I_2Gm)(BF)_2$ (**7**) with 6-ethoxy-2-naphthylboronic acid proceeds more easily and in a higher yield compared with the former process, thus giving the mono- and difunctionalized complexes $FeBd_2(EtONaphthGmH)(BF)_2$ (**2**) and $FeBd_2((EtONaphth)_2Gm)(BF)_2$ (**1**) as the products of tandem hydrodeiodination – C–C cross-coupling and double C–C cross-coupling reactions, respectively (Scheme 4). We succeeded in isolating these complexes in their individual forms and in characterizing them using various spectral and analytical methods, as well as by single crystal X-ray diffraction (see below). We suggest that the presence of the electron-donor substituent in a molecule of the above boron-containing component substantially affects the occurrence of its Suzuki–Miyaura reaction, causing an increase in the reactivity of the corresponding organopalladium intermediate.

The Sonogashira reactions of the diiodoclathrochelate precursor $FeBd_2(I_2Gm)(BF)_2$ (**7**) with trimethylsilylacetylene and acetylenecarboxylic acid as their active components in both THF and DMF media were also tested. We failed to isolate the target clathrochelate products of C–C cross-coupling in moderate yields in DMF medium due to the occurrence of a consecutive side C–C homocoupling process.[20,21] The latter copper(I)-promoted reaction of reductive dimerization is known to be affected by the reduction potential of a catalytically active copper(I) solvato-complex and, therefore, by the nature of the solvent. This potential in highly donor DMF media is substantially higher than that in THF solutions. As a result, copper(I)-promoted homocoupling and hydrodeiodination reactions of $FeBd_2(I_2Gm)(BF)_2$ (**7**) dominate over its target Sonogashira C–C cross-coupling in DMF as a solvent. This clathrochelate precursor with inherent halogen atoms was found to more easily undergo a side complete destruction reaction than its α-furyldioxime-based macrobicyclic analog shown in Scheme 2, the molecule of which bears two terminal halogen atoms (especially under basic conditions). In the case of the above Sonogashira reactions, copper(I) iodide and triethylamine were used for the activation of the corresponding ethynyl component and as an organic base, respectively. Nevertheless, the reaction

 This journal is © The Royal Society of Chemistry 2018

Open Access Article. Published on 11 April 2018. Downloaded on 7/15/2024 4:41:03 AM.
This article is licensed under a Creative Commons Attribution-NonCommercial 3.0 Unported Licence.

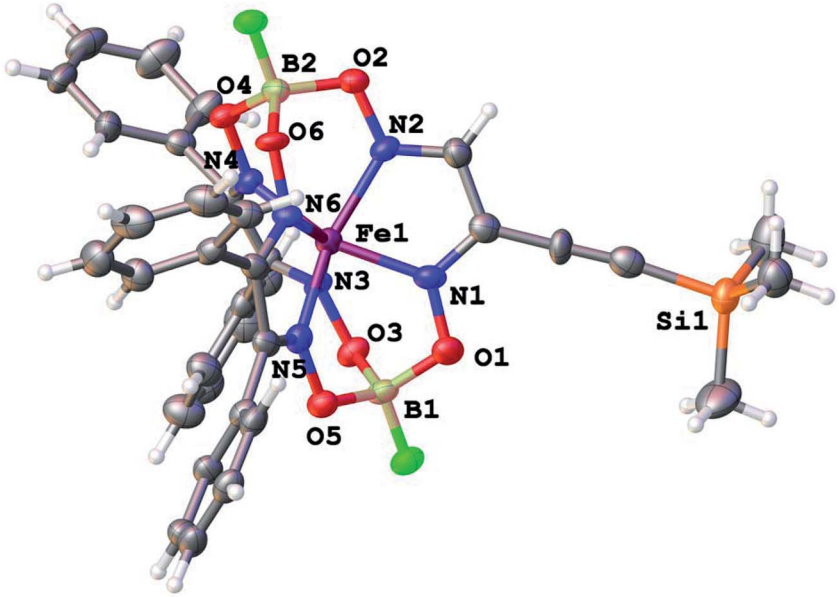

Fig. 3 General view of the molecule $FeBd_2((Me_3Si)C{\equiv}CGmH)(BF)_2$ (**4**) in a representation of its atoms with thermal ellipsoids drawn at $p = 50\%$.

of $FeBd_2(I_2Gm)(BF)_2$ (**7**), with acetylenecarboxylic acid even under the above mild conditions led to the complete destruction of its cage framework. In contrast, the tandem Sonogashira–hydrodehalogenation and double Sonogashira reactions of this diiodoclathrochelate precursor with trimethylsilylacetylene (Scheme 4) proceeded with a high total yield, giving the monofunctionalized complex $FeBd_2((Me_3Si)C{\equiv}CGmH)(BF)_2$ (**4**) as the major product, and its difunctionalized analog $FeBd_2(((Me_3Si)C{\equiv}C)_2Gm)(BF)_2$ (**3**), as a minor product. The low yield of the latter complex can be explained by its high reactivity and, therefore, by the occurrence of its further chemical transformations, plausible pathways for which are shown in Scheme 5. They include (i) cyclization giving a highly reactive biradical intermediate, that (ii) may undergo the addition of another ethynyl fragment through the corresponding C–H bond; this intermediate may also undergo further cycloaddition reactions.

Then we performed a detailed spectral and X-ray structural study of the clathrochelate products of two palladium-catalyzed Suzuki–Miyaura and Sonogashira reactions of the diiodoclathrochelate substrate $FeBd_2(I_2Gm)(BF)_2$ (**7**), in the case of which the highest yields of the target cage complexes with extended and functionalized macrobicyclic ligands were observed.

The complexes obtained were characterized using elemental analysis, MALDI-TOF mass spectrometry, UV-Vis, ^1H and $^{13}C\{^1H\}$ NMR spectra, and by single crystal X-ray diffraction (for two solvatomorphs of the dinaphthalene iron(II) clathrochelate and for a monomethinemonosilyl-containing cage complex). The most intensive peaks in the positive range of their MALDI-TOF mass spectra belong to the corresponding molecular ions.

The number and position of the signals in the solution ^1H, $^{11}B\{^1H\}$, $^{19}F\{^1H\}$ and $^{13}C\{^1H\}$ NMR spectra of the complexes synthesized, as well as the ratios of their integral intensities in ^1H NMR spectra, confirmed the composition and symmetry of the clathrochelate molecules. Nuclei of all their functionalizing groups showed the characteristic signals: in particular, the upfield signals, characteristic of the protons of trimethylsilyl groups, are observed close to the reference signal of TMS with $\delta_{^1H} = 0$ ppm. ^1H NMR spectra of the complexes $FeBd_2$(-EtONaphthGmH)$(BF)_2$ (**2**) and $FeBd_2((Me_3Si)C{\equiv}CGmH)(BF)_2$ (**4**) contain the singlet signal at approximately 8 ppm characteristic of a methine proton in their single glyoximate donor group; the multiplet signals in the range 7–8 ppm were assigned to the aromatic protons of phenyl and naphthyl ribbed substituents in a cage framework. The doublet character of the signals in the ^{11}B, ^{13}C and ^{19}F NMR spectra of these methine-containing complexes evidenced an absence of the symmetry plane passing through the middles of the chelate C–C bonds in their molecules with non-equivalent tripodal ligands' fragments.

Molecular structures of the clathrochelate $FeBd_2$((-EtONaphth)$_2$Gm)$(BF)_2$ (**1** in its two solvatomorphs) and the complex $FeBd_2((Me_3Si)C{\equiv}CGmH)(BF)_2$ (**4**) are shown in Fig. 1–3. Despite the non-equivalence of their ribbed α-dioximate fragments, the encapsulated iron(II) ion is situated almost in the centre of its FeN_6-coordination polyhedron, the geometry of which is intermediate between a trigonal prism (TP, with distortion angle $\varphi = 0°$) and a trigonal antiprism (TAP, $\varphi = 60°$); the φ values falling in the range 23.0–25.9°. The other main geometrical parameters of their cage frameworks, summarized in Table 1, are characteristic of fluoroboron-capped iron(II) tris-dioximates.[1,2] The similarity of these frameworks can be illustrated by Fig. 4, showing an overlaying of the clathrochelate molecule $FeBd_2$((EtONaphth)$_2$Gm)$(BF)_2$ (**1**) in its two X-rayed solvatomorphs. Moreover, the sterical clashes between the inherently rigid and bulky aromatic, phenyl and naphthyl ribbed substituents in a quasiaromatic macrobicyclic framework (Clt), undergoing a free rotation around the corresponding single C_{Ar}–C_{Clt} bonds, caused their very similar orientations

Open Access Article. Published on 11 April 2018. Downloaded on 7/15/2024 4:41:03 AM.
This article is licensed under a Creative Commons Attribution-NonCommercial 3.0 Unported Licence.

Table 1 Main geometrical parameters of the obtained monoribbed-functionalized iron(II) clathrochelates

Parameter	$FeBd_2((EtONaphth)_2Gm)(BF)_2$ (**1**), (in its dichloromethane solvate)	$FeBd_2((EtONaphth)_2Gm)(BF)_2$ (**1**)[a], (in its solvent–free crystal)	$FeBd_2((Me_3Si)C{\equiv}CGmH)(BF)_2$ (**4**)
Fe–N(1) (Å)	1.916(3)[b]	1.898(4)	1.915(6)[b]
Fe–N(2) (Å)	1.909(3)[b]	1.928(4)	1.935(6)[b]
Fe–N(3) (Å)	1.898(3)	1.924(4)[b]	1.906(7)
Fe–N(4) (Å)	1.909(3)		1.947(5)
Fe–N(5) (Å)	1.914(2)		1.940(6)
Fe–N(6) (Å)	1.901(2)		1.902(5)
B–O (Å)	1.481(4)–1.497(4), av. 1.489	1.489(7)–1.503(7), av. 1.496	1.479(10)–1.499(10), av. 1.487
N–O (Å)	1.369(3)–1.379(3), av. 1.375	1.3794(3)–1.386(4), av. 1.381	1.368(8)–1.394(7), av. 1.385
C=N (Å)	1.305(4)–1.317(4), av. 1.311	1.304(6)–1.329(6), av. 1.315	1.293(9)–1.324(9), av. 1.315
C–C (Å)	1.446(4)–1.458(4), av. 1.454	1.449(6)–1.449(10), av. 1.449	1.428(10)[b]–1.474(10), av. 1.451
B–F (Å)	1.361(4)–1.364(4), av. 1.363	1.355(5)	1.37(1)–1.38(1), av. 1.375
N=C–C=N (°)	6.2(6)–9.3(5), av. 7.9	8.4(7)–13.6(10), av. 10.1	6.4(8)–10.1(8), av. 7.7
φ (°)	25.9	25.4	23.0
α (°)	78.2	78.2	77.8
h (Å)	2.31	2.32	2.34

[a] Only half this molecule is symmetrically independent. [b] The distance for the functionalized ribbed chelate fragment.

against this framework. The equiprobable disordering of the functionalizing naphthalene-based *vic*-substituents over two sites in the crystal $FeBd_2((EtONaphth)_2Gm)(BF)_2$ (**1**) also suggests their free rotation around the corresponding chelate C–C bond.

Deconvolution of the UV-Vis spectra of the obtained mono- and difunctionalized iron(II) clathrochelates into their Gaussian components resulted in two or three intense metal-to-ligand charge transfer (MLCT) Fe d $\rightarrow$ Lπ^* bands in the visible range with maxima from 450 to 525 nm. Their UV-ranges contain intensive bands from 230 to 410 nm assigned to π–π^* transitions in their polyazomethine cage frameworks, as well as to those of the same nature in the ribbed aromatic and acetylene groups (fragments). The UV-vis spectrum of their clathrochelate precursor $FeBd_2(I_2Gm)(BF)_2$ (**7**) contains four MLCT bands in the visible range.[22] Thus, the substitution of two iodine atoms of this precursor by two functionalizing substituents (or by one functionalizing substituent and one hydrogen atom) led to a substantial shift in the above absorption bands, indicative of a dramatic redistribution of the electron density in a quasiaromatic clathrochelate framework caused by its ribbed functionalization with the inherent substituents in one of the three a-dioximate chelate fragments; this result is in good agreement with the above X-ray data.

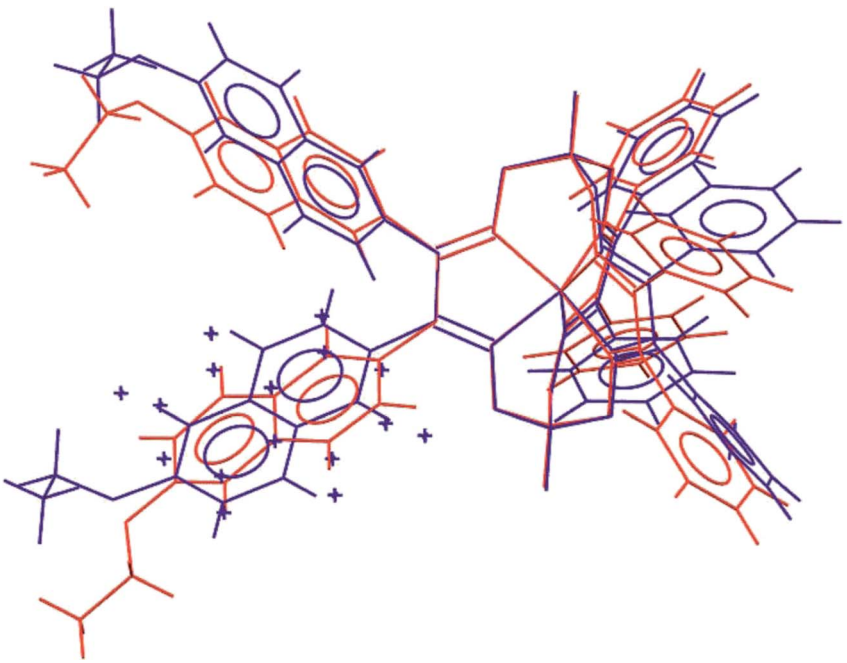

Fig. 4 Overlayed clathrochelate molecules in the solvent-containing and solvent-free solvatomorphs $FeBd_2((EtONaphth)_2Gm)(BF)_2\cdot 3CH_2Cl_2$ (**1**·$3CH_2Cl_2$, in red) and $FeBd_2((EtONaphth)_2Gm)(BF)_2$ (**1**, in blue).

 This journal is © The Royal Society of Chemistry 2018

Open Access Article. Published on 11 April 2018. Downloaded on 7/15/2024 4:41:03 AM.
This article is licensed under a Creative Commons Attribution-NonCommercial 3.0 Unported Licence.

Conclusions

Thus, the attempted palladium-catalyzed and copper-promoted Suzuki–Miyaura and Sonogashira reactions of iron(II) dihalogenoclathrochelates with inherent reactive halogen ribbed substituents were found to be strongly affected by the nature of their leaving atoms. Only a diiodomacrobicyclic complex was found to be a suitable clathrochelate substrate. Its C–C cross-coupling reactions were accompanied by the consecutive side hydrodehalogenation, C–C homocoupling and tandem hydrodehalogenation – C–C cross-coupling processes. So, the yields of the clathrochelate products of the former reactions were found to be affected by the nature of the solvent used, as well as by those of a palladium catalyst and of a base. Therefore, these reaction components, as well as the solvent and temperature, should be optimized when trying to perform the above metal-catalyzed (promoted) C–C cross-couplings in moderate if any yields.

Conflicts of interest

There are no conflicts to declare.

Acknowledgements

The synthesis of cage complexes was supported by Russian Science Foundation (grant 16-13-10475). The spectral and structural characterizations were performed with the financial support of the EU Research and Innovation Staff Exchange (RISE) (H2020-MSCA-RISE-2017, Project 'CLATHROPROBES' 778245). The XRD measurements were performed at the unique scientific facility Kurchatov Synchrotron Radiation Source supported by the Ministry of Education and Science of the Russian Federation (project code RFMEFI61917X0007). The contribution of the Center for molecule composition studies of INEOS RAS is gratefully acknowledged. Y. Z. V. and A. S. B. also thank the RFBR (grants 18-03-00675 and 17-03-00587) for the financial support. MALDI-TOF mass spectrometric measurements were performed using an equipment of CKP FMI IPCE RAS.

References

1 Y. Z. Voloshin, N. A. Kostromina and R. Krämer, *Clathrochelates: Synthesis, Structure and Properties*, Elsevier, 2002 and references therein.
2 Y. Z. Voloshin, I. G. Belaya and R. Krämer, *Cage Metal Complexes: Clathrochelates Revisited*, Springer, 2017 and references therein.
3 J. Blechinger, O. A. Varzackii, V. Kovalska, G. E. Zelinskii, Y. Z. Voloshin, E. Kinski and A. Mokhir, *Bioorg. Med. Chem. Lett.*, 2016, **26**, 626–629.
4 Y. Z. Voloshin, V. V. Novikov and Y. V. Nelyubina, *RSC Adv.*, 2015, **5**, 72621–72637.
5 O. Pantani, S. Naskar, R. Guillot, P. Millet, E. Anxolabéhère-Mallart and A. Aukauloo, *Angew. Chem., Int. Ed.*, 2008, **47**, 9948–9950.
6 E. Anxolabéhère-Mallart, C. Costentin, M. Fournier, S. Nowak, M. Robert and J. M. Savéant, *J. Am. Chem. Soc.*, 2012, **134**, 6104–6107.
7 S. El Ghachtouli, M. Fournier, S. Cherdo, R. Guillot, M. F. Charlot, E. Anxolabéhère-Mallart, M. Robert and A. Aukauloo, *J. Phys. Chem. C*, 2013, **117**, 17073–17077.
8 A. Ardavan, A. M. Bowen, A. Fernandez, A. J. Fielding, D. Kaminski, F. Moro, C. A. Muryn, M. D. Wise, A. Ruggi, E. J. L. McInnes, K. Severin, G. A. Timco, C. R. Timmel, F. Tuna, G. F. S. Whitehead and R. E. P. Winpenny, *npj Quantum Information*, 2015, **1**, 15012–15018.
9 E. J. L. McInnes, G. A. Timco, G. F. S. Whitehead and R. E. P. Winpenny, *Angew. Chem., Int. Ed.*, 2015, **54**, 14244–14269.
10 V. V. Novikov, A. A. Pavlov, Y. V. Nelyubina, M. E. Boulon, O. A. Varzatskii, Y. Z. Voloshin and R. E. P. Winpenny, *J. Am. Chem. Soc.*, 2015, **137**, 9792–9795.
11 A. A. Pavlov, Y. V. Nelyubina, S. V. Kats, L. V. Penkova, N. N. Efimov, A. O. Dmitrienko, A. V. Vologzhanina, A. S. Belov, Y. Z. Voloshin and V. V. Novikov, *J. Phys. Chem. Lett.*, 2016, **7**, 4111–4116.
12 M. D. Wise, J. J. Holstein, P. Pattison, C. Besnard, E. Solari, R. Scopelliti, G. Bricogne and K. Severin, *Chem. Sci.*, 2015, **6**, 1004–1010.
13 O. A. Varzatskii, I. N. Denisenko, S. V. Volkov, A. V. Dolganov, A. V. Vologzhanina, Y. N. Bubnov and Y. Z. Voloshin, *Inorg. Chem. Commun.*, 2013, **33**, 147–150.
14 S. V. Svidlov, O. A. Varzatskii, T. V. Potapova, A. V. Vologzhanina, S. S. Bukalov, L. A. Leites, Y. Z. Voloshin and Y. N. Bubnov, *Inorg. Chem. Commun.*, 2014, **43**, 142–145.
15 M. Wojdyr, *J. Appl. Crystallogr.*, 2010, **43**, 1126–1128.
16 G. M. Sheldrick, *Acta Crystallogr., Sect. A: Found. Adv.*, 2015, **A71**, 3–8.
17 A. L. Spek, *Acta Crystallogr., Sect. C: Struct. Chem.*, 2015, **C71**, 9–18.
18 G. M. Sheldrick, *Acta Crystallogr., Sect. C: Struct. Chem.*, 2015, **C71**, 3–8.
19 O. V. Dolomanov, L. J. Bourhis, R. J. Gildea, J. A. K. Howard and H. Puschmann, *J. Appl. Crystallogr.*, 2009, **42**, 339–341.
20 O. A. Varzatskii, V. V. Novikov, S. V. Shulga, A. S. Belov, A. V. Vologzhanina, V. V. Negrutska, I. Y. Dubey, Y. N. Bubnov and Y. Z. Voloshin, *Chem. Commun.*, 2014, **50**, 3166–3168.
21 O. A. Varzatskii, S. V. Shul'ga, A. S. Belov, V. V. Novikov, A. V. Dolganov, A. V. Vologzhanina and Y. Z. Voloshin, *Dalton Trans.*, 2014, **43**, 17934–17948.
22 Y. Z. Voloshin, A. S. Belov, O. A. Varzatskii, S. V. Shul'ga, P. A. Stuzhin, Z. A. Starikova, E. G. Lebed and Y. N. Bubnov, *Dalton Trans.*, 2012, **41**, 921–928.